TECHNICAL PAPER

Material selection for optimum design of MEMS pressure sensors

Zahid Mehmood[1,2] · Ibraheem Haneef[3] (ID) · Florin Udrea[2]

Abstract

Choice of the most suitable material out of the universe of engineering materials available to the designers is a complex task. It often requires a compromise, involving conflicts between different design objectives. Materials selection for optimum design of a Micro-Electro-Mechanical-Systems (MEMS) pressure sensor is one such case. For optimum performance, simultaneous maximization of deflection of a MEMS pressure sensor diaphragm and maximization of its resonance frequency are two key but totally conflicting requirements. Another limitation in material selection of MEMS/ Microsystems is the lack of availability of data containing accurate micro-scale properties of MEMS materials. This paper therefore, presents a material selection case study addressing these two challenges in optimum design of MEMS pressure sensors, individually as well as simultaneously, using Ashby's method. First, data pertaining to micro-scale properties of MEMS materials has been consolidated and then the Performance and Material Indices that address the MEMS pressure sensor's conflicting design requirements are formulated. Subsequently, by using the micro-scale materials properties data, candidate materials for optimum performance of MEMS pressure sensors have been determined. Manufacturability of pressure sensor diaphragm using the candidate materials, pointed out by this study, has been discussed with reference to the reported devices. Supported by the previous literature, our analysis re-emphasizes that silicon with 110 crystal orientation [Si (110)], which has been extensively used in a number of micro-scale devices and applications, is also a promising material for MEMS pressure sensor diaphragm. This paper hence identifies an unexplored opportunity to use Si (110) diaphragm to improve the performance of diaphragm based MEMS pressure sensors.

1 Introduction

Pressure sensors based upon different transduction techniques including piezoresistive (Mosser et al. 1991; Aryafar et al. 2015; Shaby et al. 2015; Rajavelu et al. 2014) (using the change in the resistance to detect strain in diaphragm-embedded strain gauges due to applied pressure), capacitive (Palasagaram and Ramadoss 2006; Rochus et al. 2016; Molla-Alipour and Ganji 2015; Sundararajan and Hasan 2014; Lei et al. 2012) (using the diaphragm deflection due to applied pressure/or pressure difference in the cavity to create a variable capacitor), resonance (Petersen et al. 1991; Burns et al. 1994; Burns et al. 1995) (measuring the change in resonance frequency of edge clamped plate/bridge due to the applied pressure), piezo-electric (Eaton and Smith 1997; Koal 1985; Sharma et al. 2012) (measuring the influence of the pressure on the charge in certain materials, such as quartz, III–V compound semiconductors and others), optical (Wagner et al. 1993; Dziuban et al. 1992; Wagner et al. 1994) (using Mach–Zehnder interferometry for measuring pressure induced deflection) and thermal (Haberli et al. 1996) (measuring the heat transfer across an air gap between source and sink based upon applied pressure) have been developed. Among these, most of the pressure sensor designs incorporate a membrane or diaphragm (as depicted in Fig. 1), whose mechanical deflection stimulates the transduction.

Membrane or diaphragm-based micro-fabricated pressure sensors are used in the medical, aerospace, process control, automation and automotive industries (Bogue

✉ Florin Udrea
  fu10000@hermes.cam.ac.uk

  Ibraheem Haneef
  ibraheem.haneef@mail.au.edu.pk

1   National University of Science and Technology, H 12, Islamabad 44000, Pakistan

2   Department of Engineering, University of Cambridge, Cambridge CB3 0FA, UK

3   Department of Mechanical and Aerospace Engineering, Institute of Avionics and Aeronautics, Air University, E-9, Islamabad 44000, Pakistan

Fig. 1 Optical micrograph (top-view) of a diaphragm based MEMS piezoresistive pressure sensor. The sensor has four piezoresistors embedded in the diaphragm (transparent membrane) to detect pressure as a function of membrane deflection

400 μm × 400 μm square membrane (diaphragm) of a MEMS pressure sensor

Piezoresistor embedded in the membrane to detect the pressure changes as a result of membrane deflection
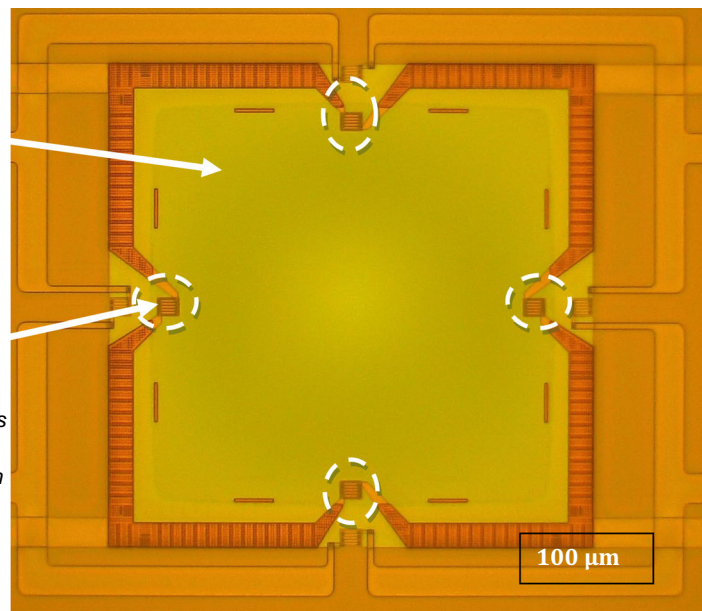
2007). Although, the very first diaphragm pressure sensor and strain gauge were reported in 1958 (Bryzek et al. 1990) and their full scale commercialization was achieved in 1990 (Bryzek 2012), yet the efforts to further improve the micro-fabricated pressure sensors' mechanical design (and hence performance) by optimizing its shape/geometrical parameters still continue. For example, the effect of diaphragm thickness and side length on sensitivity and resonant frequency were studied and it was concluded that both the sensor diaphragm and side length need to be reduced to achieve a pressure-sensitive diaphragm with high resonance frequency (Wang et al. 2006). Similarly, geometric optimization of a piezoresistive pressure sensor with measurement span of 1 MPa was also carried out for enhanced sensitivity and linearity (Ferreira et al. 2012). In this case, optimization was carried out by varying membrane thickness, edge length to thickness ratio and optimal positioning of the piezoresistive sensing elements. In another study, the effects of membrane or diaphragm thickness and edge length on pressure sensor's sensitivity were explored and a perforated membrane was proposed for improved sensitivity (Rajavelu et al. 2014). Thermal and packaging effects on the sensitivity and stability of a silicon based piezoresistive pressure sensor, caused by the geometry of silicon gel (which was used to protect the die surface) were also studied (Chou et al. 2009).

Most of the past attempts to improve the mechanical design and performance of micro-fabricated pressure sensors are primarily focused on shape or geometry optimization, and not much attention has been given to optimization of its materials. The only exceptions are papers by Spearing et al. (2000) and Qian and Zhao (2002), which report the material aspects of the mechanical design

of MEMS pressure sensors. However, the data set of the materials considered in these studies was very small. Only a total of eight and nine materials were included in their studies, respectively, and material properties considered for optimization were compared in a tabular form, mainly due to non-availability of a comprehensive MEMS materials database. Furthermore, the candidate materials for simultaneously maximizing both the key performance parameters (i.e. diaphragm deflection and resonance frequency) have never been explored or reported in the past. Maximizing both these performance requirements simultaneously is a case of conflict between the two mechanical design objectives as the material's Young's modulus is required to be maximized for achieving maximum natural frequency whereas, it is required to be minimized for achieving maximum diaphragm deflection.

In this paper, therefore, first a sizeable micro-scale properties data of MEMS materials has been consolidated. Subsequently, this data has been used along with a material selection software. Following Ashby's material selection approach (Ashby 1989; Ashby and Cebon 1993; Ashby et al. 2004; Ashby 2005), the Performance and Material Indices have been developed for a more demanding and conflicting mechanical design requirements of a MEMS pressure sensor diaphragm. In conjunction with the derived Performance and Material Indices, the consolidated materials data has been then utilized to select materials for maximizing MEMS pressure sensor diaphragm deflection and natural frequency, simultaneously. For the sake of comparison, material selection for maximizing MEMS pressure sensor diaphragm deflection and its natural resonance frequency separately has also been performed.

The structure of the remaining paper is as follows. Section 2 presents the consolidation process of MEMS materials data and its integration with the Cambridge Engineering Selector (CES) material selection software. Section 3 briefly reviews Ashby's material selection approach. Derivation of performance indices for conflicting requirements of MEMS pressure sensor diaphragm design is presented in Sect. 4. Material selection charts and candidate materials for three considered cases (i.e. maximizing only diaphragm deflection, maximizing only diaphragm resonance frequency and maximizing both diaphragm deflection and frequency simultaneously) are presented in Sect. 5. Finally, concluding remarks are given in Sect. 6.

2 MEMS materials data

A data set of micro-scale properties for MEMS materials falling in three classes i.e. (a) ceramics, (b) metals and (c) polymers, has been consolidated in Tables 1, 2, and 3, respectively. Three material properties (i.e. density, Young's modulus, and ultimate tensile strength), which are most pertinent to our study have been included in the data. For most of the MEMS materials, their properties have been reported by more than one researcher, e.g. silicon as MEMS material has been reported by 10 different researchers. Interestingly, the material properties (specifically ultimate tensile strength) of many MEMS materials vary in different papers; e.g. ultimate tensile strength of silicon by three researchers has been reported as 4000 MPa, whereas the other two reported it as 1000 MPa (ref Table 1). In such cases, where possible, ultimate tensile strength data was traced back to the specific test results. The material properties used in our data are then either taken from the reported micro-fabricated structures or from the recommended initial design values in the literature, based upon the variety of material characterization techniques. In some cases these are backed by our own experience with designing and characterization of MEMS structures.

The material properties data collected in respect of these MEMS materials was then integrated with Cambridge Engineering Selector (CES), a software developed by Granta Design (Cambridge Engineering Selector (CES), Software 1999), which is a comprehensive material selection software (Ramalhete et al. 2010).

3 Ashby's material selection methodology

In Ashby's methodology (Ashby 1989, 2005; Ashby and Cebon 1993; Ashby et al. 2004), the performance of a structural element is determined by three parameters: (1)

the functional requirements, (2) the geometry and (3) the properties of the material of which it is made. The performance P of the element is described by an equation in the form of a product as:

$$P = \left[\left(\begin{array}{c} Function \\ requirements, F \end{array} \right) \times \left(\begin{array}{c} Geometric \\ requirement, G \end{array} \right) \times \left(\begin{array}{c} Material \\ requirement, M \end{array} \right) \right] \tag{1}$$

The three parameters in Eq. (1) are independent and separable, which implies that the material requirement portion of this equation can be solved independently without solving the complete design problem or even knowing about the complete details of F and G. Therefore, from formulated performance indices (Eq. 1 above), material indices are extracted and based upon these, material selection charts are generated. The x-axis and y-axis of these material selection charts are the material properties that are aimed to be optimized. Available materials are plotted on these charts and the materials best fulfilling the selection criteria are chosen. Due to usefulness of Ashby's material selection strategy, it has not only been widely adopted in material selection for general applications and macro-systems e.g. (Ashby 1989, 2000; Ashby and Cebon 1993; Wood et al. 1997; Cebon and Ashby 1994; Huber et al. 1997) but also for a number of Microsystems/MEMS (with limited MEMS material data sets) e.g. (Sharma et al. 2012; Spearing 2000; Qian and Zhao 2002; Prasanna and Spearing 2007; Srikar and Spearing 2003a, b; Srinivasan and Spearing 2008; Pratap and Arunkumar 2007; Guisbiers et al. 2007, 2010; Guisbiers and Wautelet 2007; Reddy and Gupta 2010; Sharma and Gupta 2012; Mehmood et al. 2018).

4 Performance indices for conflicting design requirements of MEMS pressure sensor diaphragm

The main structural element of a micro-fabricated pressure sensor is its diaphragm. Such diaphragms are normally circular (Jeong 2015; Yasukawa et al. 1982) or square (Kumar and Pant 2015, 2016) (Fig. 2). In terms of shape, it is well established that for two different pressure sensors with diaphragm made of any material having same thickness and same side length or diameter, the one with square shape will experience 1.64 times higher stresses compared to the one having a circular diaphragm (Berns et al. 2006) for same applied pressure. However, material choice becomes independent of the diaphragm shape when presented in the form of Eq. (1) above. Therefore, in the current design study, we focus only on selection and

Table 1 MEMS/micro-scale material properties: ceramics

References	Materials	Density, ρ (kg/m^3)	Modulus, E (GPa)	Tensile strength, σ_f (MPa)
Spearing (2000)	Silicon	2330	129–187	4000
Qian (2002)		2330	129–187	4000
Reddy and Gupta (2010) and Parate and Gupta (2011)		NR	125–180	> 1000
Jiang and Cheung (2009)		2330	130–185	NR
Nguyen et al. (2002)		NR	200	NR
Srikar and Spearing (2003b)		NR	125–180	> 1000
Prasanna and Spearing (2007)		NR	165	NR
Rajavelu et al. (2014)		NR	106.8	NR
Yazdani and Payam (2015)		2000	160	4000
Manikam and Cheong (2011)		2330	NR	NR
Pratap and Arunkumar (2007)	Silicon (100)	2300	115–142	2000–4300
Ando et al. (2001)		NR	122	NR
Chauhan and Vaish (2012)		2300	130	3400
Pratap and Arunkumar (2007)	Silicon (110)	2300	147–188	6000–8000
Ando et al. (2001)		NR	140	NR
Chauhan and Vaish (2012)		2300	168	7000
Ando et al. (2001)	Silicon (111)	NR	111	NR
Spearing (2000)	Silicon oxide	2200	73	1000
Qian and Zhao (2002)		2200	73	1000
Prasanna and Spearing (2007)		NR	75	NR
Srikar and Spearing (2003b)		NR	70	1000
Yazdani and Payam (2015)		2000	73	1000
Pratap and Arunkumar (2007)		2500	57–92	800–1100
Reddy and Gupta (2010) and Parate and Gupta (2011)		NR	70	1000
Chauhan and Vaish (2012)		2500	70	1000
Spearing (2000)	Silicon nitride	3300	304	1000
Eaton and Smith (1997)		NR	NR	1000–2000
Qian and Zhao (2002)		3300	304	1000
Prasanna and Spearing (2007)		NR	260	NR
Srikar and Spearing (2003)		NR	250	6000
Pratap and Arunkumar (2007)		3100	230–290	5000–8000
Reddy and Gupta (2010) and Parate and Gupta (2011)		NR	250	6000
Yazdani and Payam (2015)		3000	323	1000
Sharpe et al. (2003)		NR	252–262	5830 ± 250
Chauhan and Vaish (2012)		3100	250	6400
Nguyen et al. (2002)		NR	300	NR
Spearing (2000)	Silicon carbide	3300	430	2000
Qian and Zhao (2002)		3300	430	2000
Prasanna and Spearing (2007)		NR	460	NR
Srikar and Spearing (2003b)		NR	400	NR
Reddy and Gupta (2010) and Parate and Gupta (2011)		NR	400	NR
Yazdani and Payam (2015)		3000	450	2000
Sharpe et al. (2003)		NR	417	800
Manikam and Cheong (2011)	6H-SiC	3210	NR	NR
Manikam and Cheong (2011)	3C-SiC	3170	NR	NR
Jiang and Cheung (2009)		3210	392–694	NR
Chauhan and Vaish (2012)	3H-SiC	3200	400	7000
Pratap and Arunkumar (2007)		3200	331–470	4000–9000

Table 1 continued

References	Materials	Density, ρ (kg/m^3)	Modulus, E (GPa)	Tensile strength, σ_f (MPa)
Pratap and Arunkumar (2007)	Poly-silicon	2300	140–169	1210–2800
Srikar and Spearing (2003b)		NR	160	1200–3000
Chauhan and Vaish (2012)		230	159	1650
Reddy and Gupta (2010) and Parate and Gupta (2011)		NR	160	1200–3000
Yi and Kim (1999)		NR	130–174	1250–2500
Sharpe et al. (2003)		NR	NR	3000
Franke et al. (1999)	Poly-germanium	5330	132	2200 ± 400
Koski et al. (1999)	Zirconium oxide	5130–5780	192–228	NR
Qian and Zhao (2002)	Diamond	3510	1035	1000
Spearing (2000)		3510	1035	1000
Manikam and Cheong (2011)		3520	NR	NR
Chauhan and Vaish (2012)		3500	800	8500
Yazdani and Payam (2015)		4000	1200	1000
Pratap and Arunkumar (2007)		3500	600–1100	8000–10,000
Yazdani and Payam (2015)	Titanium carbide	5000	439	NR
Qian and Zhao (2002)	Aluminum oxide	3970	393	2000
Spearing (2000)		3970	393	2000
Yazdani and Payam (2015)		4000	275	2000
Manikam and Cheong (2011)	Gallium arsenide	5320	NR	NR
Jiang and Cheung (2009)		5320	85.5	NR
Manikam and Cheong (2011)	Gallium nitride	6100	NR	NR
Phan et al. (2015)		NR	200–300	NR
Prasanna and Spearing (2007)	Diamond-like-carbon (DLC)	NR	700	NR
Srikar and Spearing (2003b)		NR	800	8000
Reddy and Gupta (2010) and Parate and Gupta (2011)		NR	800	8000
Cho et al. (2005)		NR	759 ± 22	7300 ± 1200
Santra et al. (2012)		3260	757	NR
Auciello et al. (2004)	Ultra-nano-crystalline-diamond (UNCD)	NR	980	4000–5000
Santra et al. (2012)		3500	300	NR
Espinosa et al. (2003)		NR	941–963	3950–5030
Yazdani and Payam (2015)	Quartz	3000	107	1700
Schulz (2009)	Polymer Derived ceramic (silicon carbon nitride-SiCN)	NR	150	NR
Liew et al. (2001)		2200	158	250
Qian and Zhao (2002)	Carbon single-walled nano-tubes (SWNT)	1330	> 1000	NR

NR not reported

optimization of the material of a pressure sensor diaphragm (and not its shape) for a more demanding and conflicting requirement of simultaneous maximization of both the diaphragm deflection and resonance frequency. The Performance Index for individual maximization of the diaphragm deflection is given as $M_1 = \frac{\sigma_f^{3/2}}{E}$, while that for maximization of the resonance frequency alone is reported as $M_2 = \sqrt{\frac{E}{\rho}}$ (Spearing 2000; Qian and Zhao 2002). In these Performance Indices, 'E' is the material's Young's modulus, 'ρ' is the mass density and 'σ_f' is the ultimate tensile strength, which is taken as the ultimate tensile strength of the material for all practical engineering applications.

In order to maximize M_1 index, the requirement is to select the material with maximum value of 'σ_f' and minimum value of 'E', where as for maximizing the index M_2, it is required that a material with maximum value of 'E' is

Table 2 MEMS/micro-scale material properties: metals and alloys

References	Materials	Density, ρ (kg/m^3)	Modulus, E (GPa)	Tensile strength, σ_f (MPa)
Spearing (Spearing 2000)	Nickel	8900	207	500
Qian and Zhao (2002)		8900	207	500
Prasanna and Spearing (2007)		NR	207	NR
Srikar and Spearing (2003b)		NR	180	500
Pratap and Arunkumar (2007)		8910	168–214	320–780
Guisbiers et al. (2007, 2010) and Guisbiers and Wautelet (2007)		8910	221	NR
Sharma and Gupta (2012)		NR	204	NR
Reddy and Gupta (2010) and Parate and Gupta (2011)		NR	180	500
Yazdani and Payam (2015)		8902	193	500
Yi and Kim (1999)		NR	176	560
Chauhan and Vaish (2012)		8910	185	400
Spearing (2000)	Aluminum	2710	69	300
Qian and Zhao (2002)		2710	69	300
Prasanna and Spearing (2007)		NR	68	NR
Srikar and Spearing (2003)		NR	69	150
Pratap and Arunkumar (2007)		2700	47–85	150–300
Guisbiers et al. (2007, 2010) and Guisbiers and Wautelet (2007)		2710	68	NR
Chauhan and Vaish (2012)		2700	70	170
Haque and Saif (2003)		NR	69.6–74.6	NR
Yazdani and Payam (2015)		2700	70	300
Reddy and Gupta (2010) and Parate and Gupta (2011)		NR	69	150
Sharma and Gupta (2012)		NR	69	NR
Pratap and Arunkumar (2007)	Copper	8960	86–137	120–260
Srikar and Spearing (2003b)		NR	124	350
Prasanna and Spearing (2007)		NR	110	NR
Guisbiers et al. (2007, 2010) and Guisbiers and Wautelet (2007)		8890	115	NR
Reddy and Gupta (2010) and Parate and Gupta (2011)		NR	124	350
Sharma and Gupta (2012)		NR	115	NR
Yazdani and Payam (2015)		8960	117	NR
Chauhan and Vaish (2012)		8960	120	250
Srikar and Spearing (2003b)	Gold	NR	70	300
Prasanna and Spearing (2007)		NR	77	NR
Guisbiers et al. (2007, 2010) and Guisbiers and Wautelet (2007)		19,300	75	NR
Reddy and Gupta (2010) and Parate and Gupta (2011)		NR	70	300
Sharma and Gupta (2012)		NR	77	NR
Yazdani and Payam (2015)		19,300	70	300
Guisbiers et al. (2007, 2010) and Guisbiers and Wautelet (2007)	Platinum	21,440	147	NR
Sharma and Gupta (2012)		NR	171	NR
Yazdani and Payam (2015)		21,450	168	NR
Yazdani and Payam (2015)	Titanium	4506	116	500
Guisbiers et al. (2007, 2010) and Guisbiers and Wautelet (2007)		4510	116	NR
Pratap and Arunkumar (2007)		4510	96–115	440–790
Chauhan and Vaish (2012)		4510	110	500
Yi and Kim (1999)		NR	96	950

Table 2 continued

References	Materials	Density, ρ (kg/m^3)	Modulus, E (GPa)	Tensile strength, σ_f (MPa)
Pratap and Arunkumar (2007)	Tungsten	19,300	410	700
Yazdani and Payam (2015)		19,250	411	700
Chauhan and Vaish (2012)		19,300	410	700
Yazdani and Payam (2015)	Chromium	7190	279	NR
Guisbiers et al. (2007, 2010) and Guisbiers and Wautelet (2007)		7190	289	NR
Yazdani and Payam (2015)	Silver	10,490	83	NR
Beams et al. (1952)		NR	NR	125 Approx
Yazdani and Payam (2015)	Palladium	12,023	121	NR
	Cobalt	8900	209	NR
	Iron	7874	211	NR
Srikar and Spearing (2003b)	Ni–Fe alloy	NR	120	1600
Reddy and Gupta (2010) and Parate and Gupta (2011)		NR	120	1600
Yazdani and Payam (2015)		8000	120	1600
Pornsin-Sirirak et al. (2001)	Titanium alloy (Ti–6Al–4V)	4500	110	100
Nguyen et al. (2002)	Stainless steel	NR	240	NR
Fu et al. (2001)	TiNi	NR	60–80	NR
Yazdani and Payam (2015)	Tin	7365	50	NR
Yazdani and Payam (2015)	Lead	11,340	16	NR
Sharma and Gupta (2012)	Molybdenum	NR	320	NR
Jubault et al. (2011)		10,700	NR	NR

NR not reported

selected, which is contradictory to the requirement of M$_1$. To handle these conflicting requirements, a systematic procedure has been adopted (Ashby 2005). First, the relevant performance indices have been normalized by dividing the individual index by the properties of any one selected reference/standard material (silicon in our case whose Young's modulus, ultimate tensile strength and density are denoted by E_0, σ_{f0} and ρ_0, respectively). After normalizing the indices, the problem can then be converted to the problem of minimization. The normalization of the index M$_1$ is given by Eq. (2) and for converting it into a minimization problem, its reciprocal is taken which is given by Eq. (3). Similarly, normalization and minimization of material index M$_2$ are given by Eqs. (4) and (5).

$$\frac{M_1}{M_{1,0}} = \frac{\sigma_f^{3/2}}{\sigma_{f_0}^{3/2}} \frac{E_0}{E} \tag{2}$$

$$\frac{M_{1,0}}{M_1} = \frac{\sigma_{f_0}^{3/2}}{\sigma_f^{3/2}} \frac{E}{E_0} \tag{3}$$

$$\frac{M_2}{M_{2,0}} = \sqrt{\frac{E \, \rho_0}{E_0 \, \rho}} \tag{4}$$

$$\frac{M_{2,0}}{M_2} = \sqrt{\frac{E_0 \, \rho}{E \, \rho_0}} \tag{5}$$

5 Material selection charts and candidate materials

Based upon the derived Performance Indices for the conflicting requirements of a MEMS pressure sensor's diaphragm design, material selection charts have been developed. Material properties of MEMS materials included in our MEMS materials data-base have been utilized to plot these charts. Log–log scale was used to cover the wide range of the data. Three different material selection charts with respect to three different design criteria, presented below, have been developed. Candidate materials for a variety of applications, using each design criterion, have also been elaborated.

5.1 Case 1: maximizing diaphragm deflection

The Performance Index governing the diaphragm deflection is given (Spearing 2000; Qian and Zhao 2002) as:

$$M_1 = \sigma_f^{3/2} \Big/ E \tag{6}$$

In order to achieve maximum diaphragm deflection without failure, materials with maximum value of 'σ_f' and minimum value of 'E' are required. Figure 3 is the plot of failure strength (ultimate tensile strength) 'σ_f' shown on the y-axis and Young's modulus 'E' depicted on the x-axis.

Table 3 MEMS/micro-scale material properties: polymers

References	Materials	Density, ρ (kg/m^3)	Modulus, E (GPa)	Tensile strength, σ_f (MPa)
Pratap and Arunkumar (2007)	Polyimide	1420	4–15	23–70
Prasanna and Spearing (2007)		NR	4	NR
Yazdani and Payam (2015)		1000	8	40
Chauhan and Vaish (2012)		1420	8	40
Nguyen et al. (2002)		NR	10	NR
Lorenz et al. (1997)	SU-8	NR	4.05	NR
Pratap and Arunkumar (2007)		1164	1.8–4.2	30–50
Nguyen et al. (2002)	Parylene	NR	3	NR
Pornsin-Sirirak et al. (2001)		1300	3	70
Von Metzen and Stieglitz (2013)		NR	2.9	68.9
Nguyen et al. (2002)	Silicone rubber	NR	0.0005	NR
Yang et al. (1999)		NR	0.0005	3.45
Sim et al. (2005)		1070	NR	1.57–30
Yazdani and Payam (2015)	Poly-vinylidene-di-fluoride, (PVDF)	2000	2	50
Chauhan and Vaish (2012)		1780	2.3	50
Pratap and Arunkumar (2007)		1780	1.1–4	48–60
Pratap and Arunkumar (2007)	Poly-methyl meth-acrylate (PMMA)	1200	1.8–3.1	48–80
Yazdani and Payam (2015)		1000	2	80
Wilson et al. (2007)	Poly-di-methyl-siloxane (PDMS)	NR	0.0005–0.01	4–10
Chenoweth et al. (2005)		1227	NR	NR
Wilson et al. (2007)	Poly-pyrrole (PPy)	NR	0.3–4.3	4–49
Wilson et al. (2007)	Poly-ANIline (PANI)	NR	0.1–2	0.5–50

NR not reported

Fig. 2 Typical geometry of a MEMS pressure sensor's circular and square diaphragms where a is the diaphragm's diameter (for circular membrane)/side length (for square membrane), h is the diaphragm thickness and δ_{max} is the maximum diaphragm deflection
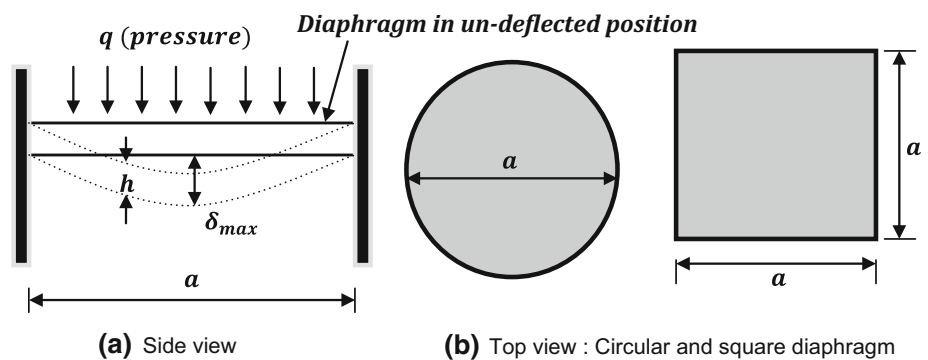
Grid lines with slope = 2/3 (by taking log of material index M_1 we get the slope of line as 2/3) were plotted on the chart. On each grid line σ_f/E has the same value; above each grid line σ_f/E has higher values, while below the grid line it has lower values.

It is evident from Fig. 3 that ceramics and polymers are promising materials for maximizing diaphragm deflection, whereas metals are comparatively less attractive. Among the ceramics silicon with crystal orientation 110 [i.e. (Si (110)] is top ranked, while from the polymers Poly-Di-Methyl-Siloxane (PDMS) and silicone rubber are the most suitable materials for applications requiring maximum deflection of pressure sensor diaphragm.

The conventionally used membrane material from ceramics i.e. Si (100) and polysilicon (Poly-Si) fall at second tier of the candidate materials identified in Fig. 3. Other ceramics materials comparable with Si (100) are silicon nitride (SiN), germanium (Ge), 3H silicon carbide (3H-SiC), diamond and Diamond Like Carbon (DLC). As such there are no MEMS devices reported in the literature
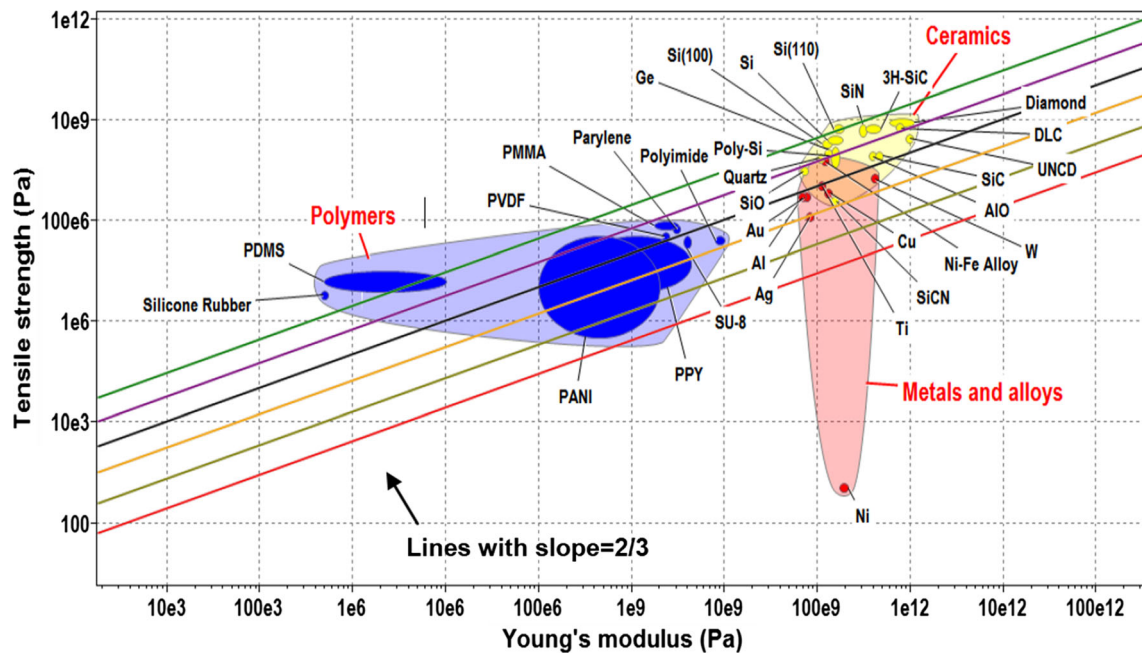
Fig. 3 MEMS pressure sensor diaphragm material selection chart for maximizing diaphragm deflection

that uses 3H-SiC, however few devices made of Ge have been reported but mostly for optoelectronics applications (Burt et al. 2017; Scopece et al. 2014). MEMS devices made of SiN, diamond and DLC and incorporating membranes for their applications are reported in the literature. However, these have been used for specific applications, details of which have been discussed in the next sections.

Similarly, polymers such as Poly-Vinyli-Dene-Fluoride (PVDF), Poly-Methyl-Meth-Acrylate) (PMMA), parylene, Polyaniline (PANI) and Polypyrrole (PPy) also fall in the second tier of the candidate materials after PDMS and silicone rubber. On the other hand, SU-8 and polyimide emerged as far inferior in terms of maximizing diaphragm deflection. Polyaniline (PANI) is suitable for gas sensing applications and its use to sense different gases has been demonstrated (Liu et al. 2009; Lee et al. 2005). Polypyrrole (PPy) is a low cost environmental friendly material that has been mainly used as an electrode material in super capacitors (Sun and Chen 2009; Sun et al. 2010; Beidaghi and Wang 2011). However, PVDF and PMMA have been used to fabricate the pressure sensor in the past. Both PVDF and PMMA have an added advantage of being biocompatible (Fung et al. 2005a, b; Shirinov and Schomburg 2008). Because of their low Young's modulus, they have a higher sensitivity compared to conventionally used Si (100); however, their pressure range is limited.

Among all these materials, the three materials i.e. Si(110), PDMS and silicone rubber that lie along the same line on the materials selection chart (i.e. green line, Fig. 3), emerge as most suitable materials since they have the same

value of index M_1. However, the final choice of the diaphragm material would depend upon the required pressure range and sensitivity of the pressure sensor.

Owing to higher values of Young's modulus, amongst the ceramics, Si (110) appears as one of the most suitable material for applications requiring measurement of higher pressures with a wider range. From micro-machining point of view, Si(110) is a CMOS compatible material and has a higher etch rate in alkali-based etchant than the conventionally used Si(100). Moreover, Si(110) surface intersects the four (111) planes at right angle, making it a suitable material for achieving structures with perfectly vertical walls (Ghodssi and Lin 2011; Lee et al. 1999), whereas such structures are not possible to achieve with Si(100) wafer using any wet etchant.

Among polymers, small stiffness values of PDMS and silicone rubber suggest them to be suitable for high sensitivity applications. Using MEMS fabrication process, membranes of silicone rubber and PDMS have been realized (Lee and Choi 2008; Yang et al. 1999).

Silicone rubber is IC compatible and exhibits excellent adhesion with CMOS compatible materials such as silicon, silicon nitride and silicon oxide. However, silicone rubber undergoes plastic deformation even with the application of small pressure (Yang et al. 1999). Moreover, its properties tend to be highly temperature dependent, which makes it very difficult to work with as a sensor (Rey et al. 2013).

PDMS, a polymer material well known for its biocompatibility and low cost, is widely used for MEMS

applications. Its usage as a membrane material in bio-compatible pressure sensors has also been widely demonstrated (Lee and Choi 2008; Liu et al. 2013; Kim and Meng 2015; Zhou et al. 2018; Xue et al. 2018; Peng et al. 2018; Chaudhury et al. 2016). One such study by Lee and Choi (2008) reported fabrication of a PDMS diaphragm pressure sensor and compared its deflection versus applied pressure curve with that of a conventional silicon [Si(100)] diaphragm pressure sensor. For the same amount of applied pressure, PDMS diaphragm underwent higher deflection than the conventional Si(100) diaphragm pressure sensor. The higher deflection of PDMS diaphragm resulted into higher sensitivity compared with the Si(100) diaphragm pressure sensor. Nevertheless, for PDMS, high volume manufacturability, long term reliability and mass production cost remain challenges to be considered, when compared to silicon.

5.2 Case 2: maximizing diaphragm resonance frequency (minimizing resonance time constant)

The Performance Index governing the resonance frequency of pressure sensor diaphragm (Spearing 2000; Qian and Zhao 2002) is $M_2 = \sqrt{E/\rho}$. To achieve maximum frequency of vibration, materials with maximum value of 'E' and minimum value of 'ρ' are required. Figure 4 is the plot of the two material properties (i.e. 'E' on the y-axis and 'ρ' on x-axis). Grid lines with slope = 1 were plotted on the chart. On each grid line, E/ρ (specific stiffness) has a constant value, the top most grid line has the highest value of E/ρ, while decreases on lower lines with the one at bottom having the lowest value.

It is evident from Fig. 4 that only ceramics are promising materials for maximizing diaphragm resonance frequency, whereas metals and polymers are comparatively less attractive. Among the ceramics, diamond, Diamond Like Carbon (DLC) and Ultra Nano Crystalline Diamond (UNCD) are the preferred materials for pressure sensor diaphragm intended to be used for high frequency pressure measurement applications.

At the second tier of Fig. 4, materials such as silicon carbide (SiC), 3H-SiC, SiN and aluminum oxide (AlO) also appear as potential candidate materials for high frequency applications. Aluminum oxide is mainly being used as a humidity sensor (Lan et al. 2018; Kim et al. 2009; Nahar 2000); however, due to its high specific stiffness (E/ρ) it can potentially be used for high frequency applications as well (Spearing 2000). Similar to aluminum oxide, SiC also has high specific stiffness. Additionally, it also has high thermal conductivity, high electric field breakdown strength and wide band-gap, making it a good candidate material for high temperature, high power and high frequency applications (Casady and Johnson 1996). To exploit all these advantages, SiC pressure sensors have been developed for applications in harsh environment (Wieczorek et al. 2007; Beker et al. 2017).

Figure 4 also depicts that diamond, Diamond Like Carbon (DLC) and Ultra Nano Crystalline Diamond (UNCD) are even better than silicon carbide for high frequency applications.

Diamond and DLC can be deposited in the form of thin films using a variety of deposition techniques such as plasma enhanced chemical vapor deposition, plasma assisted chemical vapor deposition, microwave plasma chemical vapor deposition, ion beam deposition, pulsed laser ablations, filtered cathodic arc deposition, magnetron sputtering and DC plasma-jet chemical vapor deposition (Boudina et al. 1992; Fu et al. 2000; Santra et al. 2012). Though the deposition of diamond and DLC include some inherent issues such as high deposition temperature (600–1000 °C), large intrinsic and thermal stresses, low deposition rates, poor adhesion to substrate and higher values of surface roughness (Luo et al. 2007), yet the use of diamond in high frequency applications (Baliga 1989; Taniuchi et al. 2001) and realization of its membranes has been demonstrated (Davidson et al. 1999; Kohn et al. 1999). Pressure sensors made of all diamond (i.e. both membranes and piezoresistors are made of diamond) have also been fabricated and characterized (Wur et al. 1995; Davidson et al. 1996).

In spite of successful demonstration of diamond and DLC in high frequency measurement applications, their deposition related issues restrict the exploitation of full benefits of diamond and DLC in wider MEMS applications. Many of these issues were however, resolved in UNCD film technology developed by Argonne National Laboratory (Auciello et al. 2004), rendering UNCD also a promising MEMS materials for high frequency applications. The developed UNCD films have been successfully implemented to form wide dynamic range pressure, acceleration and vibration sensors (Krauss et al. 2002).

5.3 Case 3: simultaneous maximization of diaphragm deflection and vibration frequency

The material selection chart for selecting optimized materials considering both the design requirements (i.e. maximum deflection and maximum frequency) of MEMS pressure sensor diaphragm is given in Fig. 5. In this figure, Eq. (3) has been plotted on the y-axis, while Eq. (5) is on the x-axis. Figure 5 has been divided into four sectors, with point (1,1) corresponding to silicon being in the center,
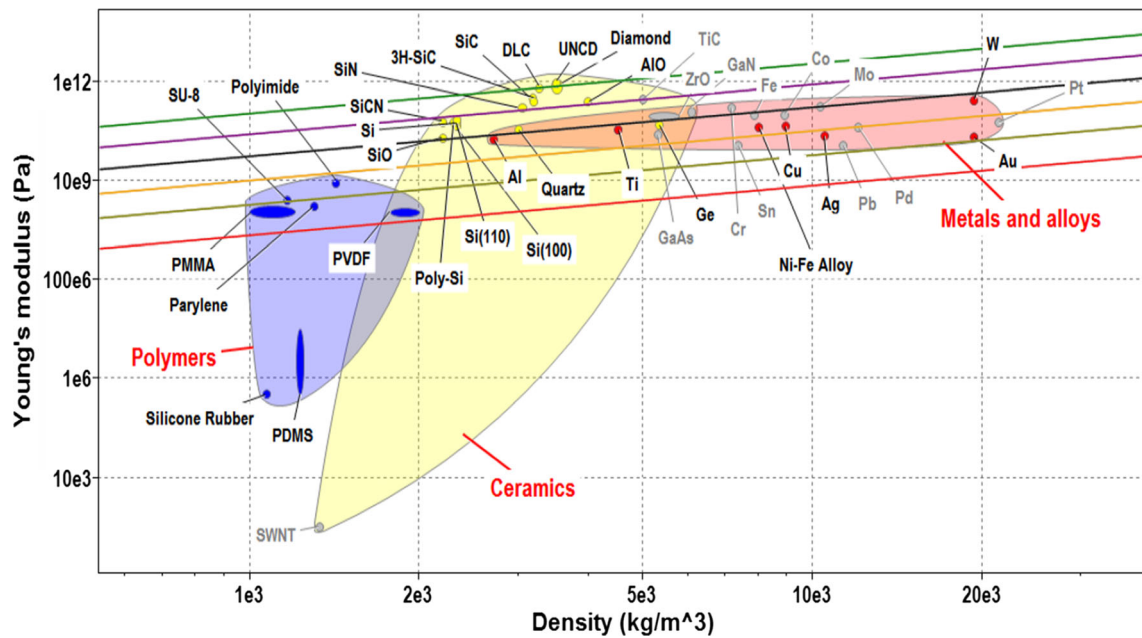
Fig. 4 MEMS pressure sensor diaphragm material selection chart for maximizing diaphragm resonance frequency (or minimizing vibration time constant)

which has been selected as reference material for comparison. The materials falling in sector A are the best materials having both the performance parameters (i.e. deflection and frequency) at maximum and superior to silicon. Materials falling in sector B, C and D have performance, in terms of both deflection and frequency, inferior to that of silicon with materials in sector C being the least promising.

Figure 5 reveals that when both diaphragm deflection and its resonance frequency are required to be maximized simultaneously, then ceramics are the most promising candidate materials, while metals and polymers are far inferior to ceramics. Figure 5 also reveals that 3H-SiC, silicon nitride (SiN) and (110) oriented silicon [i.e. Si(110)] are the only three materials, which would perform better than most frequently reported silicon diaphragm based MEMS pressure sensors.

Interestingly, UNCD (that previously emerged as the most suitable material for high frequency applications of pressure sensor) and PDMS (which previously emerged as the most suitable material for large deflection applications of pressure sensor) have inferior performance, when both diaphragm deflection and frequency are required to be maximized simultaneously. However, Si (110), which emerged as the most suitable material for applications requiring large deflections, is still a candidate material for maximizing both deflection and frequency simultaneously. The other preferred material in this case is silicon nitride. 3H-SiC is also depicted to be a promising material in this

case. However, as mentioned earlier, no 3H-SiC based MEMS devices have yet been reported.

While both Si(110) and SiN are CMOS compatible materials, Si(110) has a number of unique advantages: (a) it is mechanically superior than Si (100), (b) it has higher etch rate in Alkali-based etchant than the conventionally used Si (100), (c) its surface intersects the four (111) planes at right angle making it a suitable material for achieving structures with perfectly vertical walls (Ghodssi and Lin 2011; Lee et al. 1999), (d) the maximum longitudinal piezoresistance coefficient is along <111> direction, which is on silicon (110) plane. Kanda et al. (Kanda and Yasukawa 1997) showed that when the non-linearity and the full scale pressure are the same, the sensitivity of a piezoresistor pressure sensor on Si(110) wafer is 1.4 times higher than that of the conventionally used Si(100) wafer. The only disadvantage associated with Si (110) oriented wafer is that rectangular-bottom cavities cannot be achieved using wet etchant as two of (111) planes intersect Si(110) plane perpendicularly at an angle of 109.48° and remaining two intersect Si(110) plane surface at an angle of 35.26° (Bassous 1978). However, this limitation has been overcome by using more advanced etching techniques such as deep reactive ion etching (DRIE). This has been demonstrated experimentally by Lee et al. (Lee et al. 2009) whereby 100 μm tall vertical mirrors were fabricated using a combination of KOH etch and DRIE.

The findings of our current study and the past literature (Kanda and Yasukawa 1997) suggest that Si(110) has a good potential to increase the sensitivity of a diaphragm
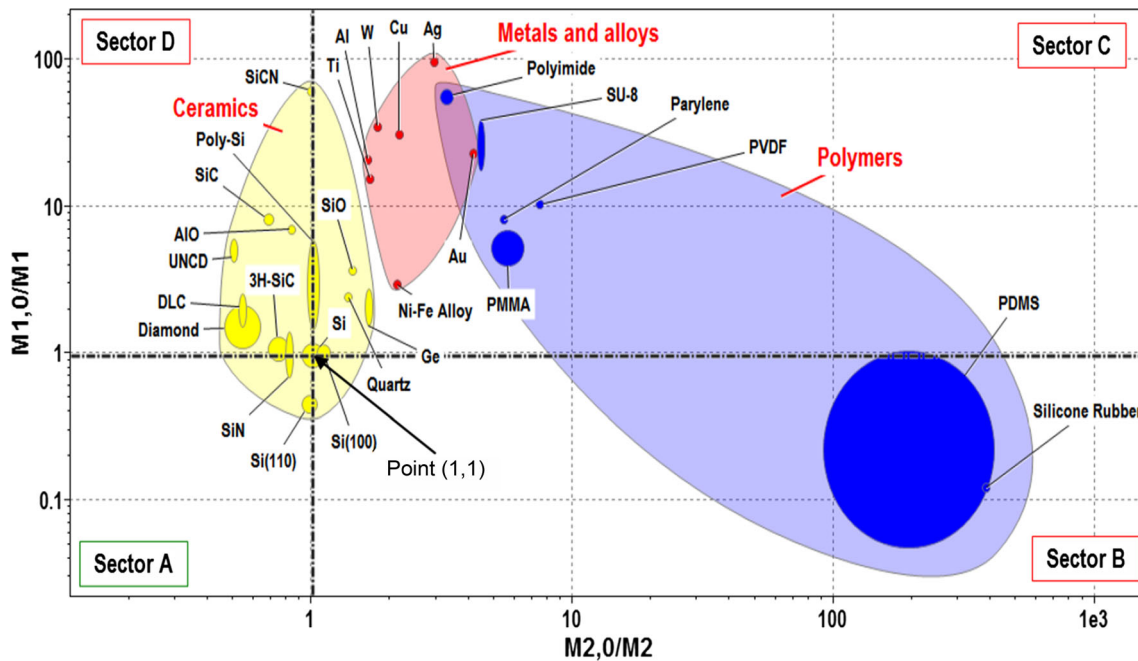
Fig. 5 MEMS pressure sensor diaphragm material selection chart for simultaneously maximization of both the diaphragm deflection and its vibration frequency

pressure sensor, which has yet not been exploited. It is worth mentioning that Si(110) is an active research area (Rao et al. 2017; Dutta et al. 2011; Hölke and Henderson 1999; Singh et al. 2017; Swarnalatha et al. 2018) and already being used for fabrication of various micro-machined/MEMS devices. Examples of Si(110) wafer based micro-machined devices include a high aspect ratio comb actuator (Kim et al. 2002), a high sensitivity vertical hall sensor (Chiu et al. 2001), a capacitive accelerometer for air bag application (Tsugai et al. 1997), an opto-mechanical accelerometer based on strain sensing by a Bragg grating in a planar waveguide (Storgaard-Larsen et al. 1996), a vertical-membrane optical-fiber pressure sensor (Tu and Zemel 1993), a micro-channel (Singh et al. 2008) and an optical Fabry–Perot modulator (Chaffey et al. 2004) etc.

On the other hand, pressure sensors having silicon nitride (SiN) membranes have also been demonstrated (Kumar and Pant 2015). Using silicon nitride as a membrane material is advantageous in a sense that it has a higher strength than the conventionally used Si(100) membrane. Folkmer et al. (Folkmer et al. 1996) conducted a blister test on membranes made of conventional silicon, silicon carbide and silicon nitride. They demonstrated that silicon nitride membrane has the highest strength (maximum pressure taking capability). However, random crystalline orientation, smaller crystalline grain size and presence of high residual stresses in the SiN are the issues (Eaton et al. 1999; Sugiyama et al. 1986) to be catered while using it as diaphragm material in pressure sensors.

6 Conclusions

Material selection for MEMS based pressure sensor, taking into account the demanding and conflicting requirement of simultaneously maximizing its diaphragm deflection and natural frequency of vibration, has been reported for the first time. Since no comprehensive MEMS materials database incorporating micro-scale properties was readily available, first a MEMS specific materials data is consolidated, which included three key properties (i.e. density, Young's modulus and ultimate tensile strength) at micro-scale for ceramics (Table 1), metals and alloys (Table 2) and polymers (Table 3) reported in the literature. This data has been then successfully integrated with a material selection software, CES (Cambridge Engineering Selector), to develop material selection charts.

Based upon the formulated Performance Indices, the performance of MEMS materials included in the consolidated MEMS micro-scale properties data has been analyzed for three different design requirements of pressure sensor. The materials, which emerge as the most suitable materials for these design requirements are further critically analyzed in light of microfabrication processes available for them. Amongst the candidate materials whose microfabrication or application in micro-sensors has been previously demonstrated, the most promising materials have been identified for the three design conditions requirements in this study.

Our analysis suggests that PDMS is a promising material to be used for pressure sensor diaphragms requiring large deflection, high sensitivity as well as bio-compatibility. If the aim is to achieve only a high frequency response, then UNCD is the best material. Silicon with crystal orientation 110 [i.e. Si(110)] emerged as most suited material capable of fulfilling two distinct design requirement of MEMS pressure sensor diaphragms: (a) for pressure sensors requiring only maximum diaphragm deflection (and sensitivity) for measurement of high pressures over wide pressure ranges. (b) for simultaneously achieving highest deflection (sensitivity) and highest frequency response of diaphragm. This is in close agreement with the fact highlighted previously that the performance of conventional silicon pressure sensor can be increased by a factor of 1.4 if Si(100) diaphragm is replaced with the Si(110) diaphragm.

This study has hence identified an opportunity for MEMS designers and researchers to exploit the Si(110) diaphragm based pressure sensors for achieving improved pressure measurement range, higher frequency and higher sensitivity compared to the Si(100) based MEMS pressure sensors.

The material selection methodology and the MEMS materials data with micro-scale material properties reported in this design case study is not only limited for selection of materials for MEMS pressure sensors but can also be applied for systematic and successful material selection of other MEMS devices.

References

Ando T, Shikida M, Sato K (2001) Tensile-mode fatigue testing of silicon films as structural materials for MEMS. Sens Actuators A 93(1):70–75

Aryafar M, Hamedi M, Ganjeh MM (2015) A novel temperature compensated piezoresistive pressure sensor. Measurement 63:25–29

Ashby M (1989) Materials selection in conceptual design. Mater Sci Technol 5(6):517–525

Ashby M (2000) Multi-objective optimization in material design and selection. Acta Mater 48(1):359–369

Ashby MF (2005) Materials selection in mechanical design. Pergamon Press, Oxford

Ashby MF, Cebon D (1993) Materials selection in mechanical design. J de Phys IV 3(C7):C7-1– C7-9

Ashby M, Brechet Y, Cebon D, Salvo L (2004) Selection strategies for materials and processes. Mater Des 25(1):51–67

Auciello O, Birrell J, Carlisle JA, Gerbi JE, Xiao X, Peng B, Espinosa HD (2004) Materials science and fabrication processes for a new MEMS technology based on ultrananocrystalline diamond thin films. J Phys: Condens Matter 16(16):R539

Baliga BJ (1989) Power semiconductor device figure of merit for high-frequency applications. IEEE Electron Device Lett 10(10):455–457

Bassous E (1978) Fabrication of novel three-dimensional microstructures by the anisotropic etching of (100) and (110) silicon. IEEE Trans Electron Devices 25(10):1178–1185

Beams J, Walker W, Morton H Jr (1952) Mechanical properties of thin films of silver. Phys Rev 87(3):524

Beidaghi M, Wang C (2011) Micro-supercapacitors based on three dimensional interdigital polypyrrole/C-MEMS electrodes. Electrochim Acta 56(25):9508–9514

Beker L, Maralani A, Lin L, Pisano AP (2017) A silicon carbide differential output pressure sensor by concentrically matched capacitance. In: 30th IEEE international conference on micro electro mechanical systems (MEMS'17). 2017

Berns A, Buder U, Obermeier E, Wolter A, Leder A (2006) AeroMEMS sensor array for high-resolution wall pressure measurements. Sens Actuators A 132(1):104–111

Bogue R (2007) MEMS sensors: past, present and future. Sens Revi 27(1):7–13

Boudina A, Fitzer E, Wahl G (1992) Diamond film preparation by arc-discharge plasma-jet-CVD and thermodynamic calculation of the equilibrium gas composition. Diam Relat Mater 1(2–4):380–387

Bryzek J (2012) Roadmap to a $ trillion MEMS market. In: 10th annual MEMS technology symposium. 2012. California, USA

Bryzek J, Peterson K, Mallon J Jr, Christel L, Pourahamadi F (1990) Silicon sensors and microstructures. Nova Sensor, Silicon Valley

Burns D, Zook J, Horning R, Herb W, Guckel H (1994) A digital pressure sensor based on resonant microbeams. In: Proceedings of the solid-state sensor and actuator workshop. 1994

Burns D, Zook J, Horning R, Herb W, Guckel H (1995) Sealed-cavity resonant microbeam pressure sensor. Sens Actuators A 48(3):179–186

Burt D, Al-Attili A, Li Z, Liu F, Oda K, Higashitarumizu N, Ishikawa Y, Querin O, Gardes F, Kelsall R (2017) Strain-engineering in germanium membranes towards light sources on Silicon. In: IEEE conference on electron devices technology and manufacturing (EDTM'17). 2017

Cambridge Engineering Selector (CES), Software (1999) Granta design, Cambridge, UK

Casady J, Johnson RW (1996) Status of silicon carbide (SiC) as a wide-bandgap semiconductor for high-temperature applications: a review. Solid-State Electron 39(10):1409–1422

Cebon D, Ashby N (1994) Materials selection for precision instruments. Meas Sci Technol 5(3):296

Chaffey JP, Austin M, Switala I (2004) Bulk micromachined optical Fabry-Perot modulator. In: Photonics: design, technology, and packaging, international society for optics and photonics. 2004

Chaudhury A, Pantazis A, Chronis N (2016) An image contrast-based pressure sensor. Sens Actuators A 245:63–67

Chauhan A, Vaish R (2012) A comparative study on material selection for micro-electromechanical systems. Mater Des 41:177–181

Chenoweth K, Cheung S, van Duin AC, Goddard WA, Kober EM (2005) Simulations on the thermal decomposition of a poly (dimethylsiloxane) polymer using the ReaxFF reactive force field. J Am Chem Soc 127(19):7192–7202

Chiu HW, Lu S, Lan H (2001) Vertical hall sensor of high sensitivity and excellent confinement fabricated on the (110) silicon substrate. In: MEMS design, fabrication, characterization, and packaging, international society for optics and photonics 2001

Cho S, Chasiotis I, Friedmann TA, Sullivan JP (2005) Young's modulus, Poisson's ratio and failure properties of tetrahedral amorphous diamond-like carbon for MEMS devices. J Micromech Microeng 15(4):728

Chou T-L, Chu C-H, Lin C-T, Chiang K-N (2009) Sensitivity analysis of packaging effect of silicon-based piezoresistive pressure sensor. Sens Actuators A 152(1):29–38

Davidson J, Wur D, Kang W, Kinser D, Kerns D (1996) Polycrystalline diamond pressure microsensor. Diam Relat Mater 5(1):86–92

Davidson J, Kang W, Gurbuz Y, Holmes K, Davis L, Wisitsora-At A, Kerns D, Eidson R, Henderson T (1999) Diamond as an active sensor material. Diam Relat Mater 8(8–9):1741–1747

Dutta S, Imran M, Kumar P, Pal R, Datta P, Chatterjee R (2011) Comparison of etch characteristics of KOH, TMAH and EDP for bulk micromachining of silicon (110). Microsyst Technol 17(10–11):1621

Dziuban J, Gorecka-Drzazga A, Lipowicz U (1992) Silicon optical pressure sensor. Sens Actuators A 32(1):628–631

Eaton WP, Smith JH (1997) Micromachined pressure sensors: review and recent developments. Smart Mater Struct 6:30–41

Eaton WP, Bitsie F, Smith JH, Plummer DW (1999) A new analytical solution for diaphragm deflection and its application to a surface-micromachined pressure sensor. In: International conference on modeling and simulation of microsystems, USA

Espinosa H, Prorok B, Peng B, Kim K, Moldovan N, Auciello O, Carlisle J, Gruen D, Mancini D (2003) Mechanical properties of ultrananocrystalline diamond thin films relevant to MEMS/NEMS devices. Exp Mech 43(3):256–268

Ferreira C, Grinde C, Morais R, Valente A, Neves C, Reis M (2012) Optimized design of a piezoresistive pressure sensor with measurement span of 1.0 MPa. Proc Eng 47:1307–1310

Folkmer B, Steiner P, Lang W (1996) A pressure sensor based on a nitride membrane using single-crystalline piezoresistors. Sens Actuators A 54(1–3):488–492

Franke A, Bilic D, Chang D, Jones P, King TJ, Howe R, Johnson G (1999) Post-CMOS integration of germanium microstructures. In: 12th IEEE international conference on micro-electro-mechanical-systems (MEMS'99)

Fu Y, Yan B, Loh NL, Sun CQ, Hing P (2000) Characterization and tribological evaluation of MW-PACVD diamond coatings deposited on pure titanium. Mater Sci Eng, A 282(1):38–48

Fu Y, Huang W, Du H, Huang X, Tan J, Gao X (2001) Characterization of TiNi shape-memory alloy thin films for MEMS applications. Surf Coat Technol 145(1–3):107–112

Fung CK, Zhang MQ, Dong Z, Li WJ (2005a) Fabrication of CNT-based MEMS piezoresistive pressure sensors using DEP nanoassembly. In: 5th IEEE conference on nanotechnology 2005

Fung CK, Zhang MQ, Chan RH, Li WJ (2005b) A PMMA-based micro pressure sensor chip using carbon nanotubes as sensing elements. In: 18th IEEE international conference on micro electro mechanical systems (MEMS'05) 2005

Ghodssi R, Lin P (2011) MEMS materials and processes handbook, vol 1. Springer, Berlin

Guisbiers G, Wautelet M (2007) Materials selection for micro-electromechanical systems. Mater Des 28(1):246–248

Guisbiers G, Van Overschelde O, Wautelet M (2007) Materials selection for thin films for radio frequency microelectromechanical systems. Mater Des 28(6):1994–1997

Guisbiers G, Herth E, Legrand B, Rolland N, Lasri T, Buchaillot L (2010) Materials selection procedure for RF-MEMS. Microelectron Eng 87(9):1792–1795

Haberli A, Paul O, Malcovati P, Faccio M, Maloberti E, Baltes H (1996) CMOS integration of a thermal pressure sensor system. In: IEEE international symposium on circuits and systems (ISCAS'96)

Haque M, Saif M (2003) A review of MEMS-based microscale and nanoscale tensile and bending testing. Exp Mech 43(3):248–255

Hölke A, Henderson HT (1999) Ultra-deep anisotropic etching of (110) silicon. J Micromech Microeng 9(1):51

Huber J, Fleck N, Ashby M (1997) The selection of mechanical actuators based on performance indices. In: Proceedings of the royal society of London A: mathematical, physical and engineering sciences. 1997: The Royal Society

Jeong T (2015) Design and modeling of sensor behavior for improving sensitivity and performance. Measurement 62:230–236

Jiang L, Cheung R (2009) A review of silicon carbide development in MEMS applications. Int J Comput Mater Sci Surf Eng 2(3–4):227–242

Jubault M, Ribeaucourt L, Chassaing E, Renou G, Lincot D, Donsanti F (2011) Optimization of molybdenum thin films for electrodeposited CIGS solar cells. Sol Energy Mater Sol Cells 95:S26–S31

Kanda Y, Yasukawa A (1997) Optimum design considerations for silicon piezoresistive pressure sensors. Sens Actuators A 62(1–3):539–542

Kim BJ, Meng E (2015) Review of polymer MEMS micromachining. J Micromech Microeng 26(1):013001

Kim S-H, Lee S-H, Kim Y-K (2002) A high-aspect-ratio comb actuator using UV-LIGA surface micromachining and (110) silicon bulk micromachining. J Micromech Microeng 12(2):128

Kim Y, Jung B, Lee H, Kim H, Lee K, Park H (2009) Capacitive humidity sensor design based on anodic aluminum oxide. Sens Actuators B Chem 141(2):441–446

Koal JG (1985) Polymer piezoelectric sensor of animal foot pressure. Google Patents (US Patent No. US4499394 A)

Kohn E, Gluche P, Adamschik M (1999) Diamond MEMS—a new emerging technology. Diam Relat Mater 8(2–5):934–940

Koski K, Hölsä J, Juliet P (1999) Properties of zirconium oxide thin films deposited by pulsed reactive magnetron sputtering. Surf Coat Technol 120:303–312

Krauss AR, Gruen DM, Pellin MJ, Auciello O (2002) Ultrananocrystalline diamond cantilever wide dynamic range acceleration/vibration/pressure sensor. Argonne National Laboratory (ANL), Argonne

Kumar SS, Pant B (2015a) Polysilicon thin film piezoresistive pressure microsensor: design, fabrication and characterization. Microsyst Technol 21(9):1949–1958

Kumar SS, Pant B (2015) Fabrication and characterization of pressure sensor, and enhancement of output characteristics by modification of operating pressure range. In: 19th IEEE international symposium on VLSI design and test (VDAT) 2015

Kumar SS, Pant B (2016) Effect of piezoresistor configuration on output characteristics of piezoresistive pressure sensor: an experimental study. Microsyst Technol 22(4):709–719

Lan D, Zhao X, Wang F, Ai C, Wen D, Zhang H (2018) Fabrication and characteristics of the high-sensitivity humidity sensor of

anodic aluminum oxide based on silicon substrates. Int J Mod Phys B 1850:199

Lee D-W, Choi Y-S (2008) A novel pressure sensor with a PDMS diaphragm. Microelectron Eng 85(5–6):1054–1058

Lee S, Park S, Cho D-I (1999) The surface/bulk micromachining (SBM) process: a new method for fabricating released MEMS in single crystal silicon. J Microelectromech Syst 8(4):409–416

Lee Y-S, Song K-D, Huh J-S, Chung W-Y, Lee D-D (2005) Fabrication of clinical gas sensor using MEMS process. Sens Actuators B Chem 108(1–2):292–297

Lee D, Yu K, Krishnamoorthy U, Solgaard O (2009) Vertical mirror fabrication combining KOH etch and DRIE of (110) silicon. J Microelectromech Syst 18(1):217–227

Lei KF, Lee K-F, Lee M-Y (2012) Development of a flexible PDMS capacitive pressure sensor for plantar pressure measurement. Microelectron Eng 99:1–5

Liew L-A, Zhang W, Bright VM, An L, Dunn ML, Raj R (2001) Fabrication of SiCN ceramic MEMS using injectable polymer-precursor technique. Sens Actuators A 89(1–2):64–70

Liu M-C, Dai C-L, Chan C-H, Wu C-C (2009) Manufacture of a polyaniline nanofiber ammonia sensor integrated with a readout circuit using the CMOS–MEMS technique. Sensors 9(2):869–880

Liu X, Zhu Y, Nomani MW, Wen X, Hsia T-Y, Koley G (2013) A highly sensitive pressure sensor using a Au-patterned poly-dimethylsiloxane membrane for biosensing applications. J Micromech Microeng 23(2):025022

Lorenz H, Despont M, Fahrni N, LaBianca N, Renaud P, Vettiger P (1997) SU-8: a low-cost negative resist for MEMS. J Micromech Microeng 7(3):121

Luo J, Fu YQ, Le H, Williams JA, Spearing S, Milne W (2007) Diamond and diamond-like carbon MEMS. J Micromech Microeng 17(7):S147

Manikam VR, Cheong KY (2011) Die attach materials for high temperature applications: a review. IEEE Trans Compon Pack Manuf Technol 1(4):457–478

Mehmood Z, Haneef I, Udrea F (2018) Material selection for micro-electro-mechanical-systems (MEMS) using Ashby's approach. Mater Des 157:412–430

Molla-Alipour M, Ganji BA (2015) Analytical analysis of MEMS capacitive pressure sensor with circular diaphragm under dynamic load using differential transformation method (DTM). Acta Mech Solida Sin 28(4):400–408

Mosser V, Suski J, Goss J, Obermeier E (1991) Piezoresistive pressure sensors based on polycrystalline silicon. Sens Actuators A 28(2):113–132

Nahar R (2000) Study of the performance degradation of thin film aluminum oxide sensor at high humidity. Sens Actuators B Chem 63(1–2):49–54

Nguyen N-T, Huang X, Chuan TK (2002) MEMS-micropumps: a review. J Fluids Eng 124(2):384–392

Palasagaram JN, Ramadoss R (2006) MEMS-capacitive pressure sensor fabricated using printed-circuit-processing techniques. IEEE Sens J 6(6):1374–1375

Parate O, Gupta N (2011) Material selection for electrostatic microactuators using Ashby approach. Mater Des 32(3):1577–1581

Peng Y, Wang T, Jiang W, Liu X, Wen X, Wang G (2018) Modeling and optimization of inductively coupled wireless bio-pressure sensor system using the design of experiments method. IEEE Trans Compon Pack Manuf Technol 8(1):65–72

Petersen K, Pourahmadi F, Brown J, Parsons P, Skinner M, Tudor J (1991) Resonant beam pressure sensor fabricated with silicon fusion bonding. In: IEEE international conference on solid-state sensors and actuators

Phan H-P, Dao DV, Nakamura K, Dimitrijev S, Nguyen N-T (2015) The piezoresistive effect of SiC for MEMS sensors at high temperatures: a review. J Microelectromech Syst 24(6):1663–1677

Pornsin-Sirirak TN, Tai Y, Nassef H, Ho C (2001) Titanium-alloy MEMS wing technology for a micro aerial vehicle application. Sens Actuators A 89(1–2):95–103

Prasanna S, Spearing SM (2007) Materials selection and design of microelectrothermal bimaterial actuators. J Microelectromech Syst 16(2):248–259

Pratap R, Arunkumar A (2007) Material selection for MEMS devices. Indian J Pure Appl Phys 45(4):358–367

Qian J, Zhao Y-P (2002) Materials selection in mechanical design for microsensors and microactuators. Mater Des 23(7):619–625

Rajavelu M, Sivakumar D, Joseph Daniel R, Sumangala K (2014) Perforated diaphragms employed piezoresistive MEMS pressure sensor for sensitivity enhancement in gas flow measurement. Flow Meas Instrum 35:63–75

Ramalhete P, Senos A, Aguiar C (2010) Digital tools for material selection in product design. Mater Des 31(5):2275–2287

Rao AN, Swarnalatha V, Pal P (2017) Etching characteristics of Si 110 in 20 wt% KOH with addition of hydroxylamine for the fabrication of bulk micromachined MEMS. Micro Nano Syst Lett 5(1):23

Reddy PG, Gupta N (2010) Material selection for microelectronic heat sinks: an application of the Ashby approach. Mater Des 31(1):113–117

Rey T, Chagnon G, Le Cam J-B, Favier D (2013) Influence of the temperature on the mechanical behaviour of filled and unfilled silicone rubbers. Polym Test 32(3):492–501

Rochus V, Wang B, Tilmans HAC, Ray Chaudhuri A, Helin P, Severi S, Rottenberg X (2016) Fast analytical design of MEMS capacitive pressure sensors with sealed cavities. Mechatronics 40:244–250

Santra T, Bhattacharyya T, Patel P, Tseng F, Barik T (2012) Diamond, diamond-like carbon (DLC) and diamond-like nanocomposite (DLN) thin films for MEMS applications. In: Microelectromechanical systems and devices (Book Section). 2012, InTech

Schulz M (2009) Polymer derived ceramics in MEMS/NEMS—a review on production processes and application. Adv Appl Ceram 108(8):454–460

Scopece D, Montalenti F, Bollani M, Chrastina D, Bonera E (2014) Straining Ge bulk and nanomembranes for optoelectronic applications: a systematic numerical analysis. Semicond Sci Technol 29(9):095012

Shaby SM, Premi MG, Martin B (2015) Enhancing the performance of MEMS piezoresistive pressure sensor using Germanium nanowire. Proc Mater Sci 10:254–262

Sharma AK, Gupta N (2012) Material selection of RF-MEMS switch used for reconfigurable antenna using Ashby's Methodology. Prog Electromagn Res Lett 31:147–157

Sharma T, Je S-S, Gill B, Zhang JX (2012) Patterning piezoelectric thin film PVDF–TrFE based pressure sensor for catheter application. Sens Actuators A 177:87–92

Sharpe W, Bagdahn J, Jackson K, Coles G (2003) Tensile testing of MEMS materials: recent progress. J Mater Sci 38(20):4075–4079

Shirinov A, Schomburg W (2008) Pressure sensor from a PVDF film. Sens Actuators A 142(1):48–55

Sim LC, Ramanan S, Ismail H, Seetharamu K, Goh T (2005) Thermal characterization of Al_2O_3 and ZnO reinforced silicone rubber as thermal pads for heat dissipation purposes. Thermochim Acta 430(1–2):155–165

Singh S, Kulkarni A, Duttagupta S, Puranik B, Agrawal A (2008) Impact of aspect ratio on flow boiling of water in rectangular microchannels. Exp Thermal Fluid Sci 33(1):153–160

Singh S, Avvaru V, Veerla S, Pandey AK, Pal P (2017) A measurement free pre-etched pattern to identify the <110> directions on Si 110 wafer. Microsyst Technol 23(6):2131–2137

Spearing SM (2000) Materials issues in microelectromechanical systems (MEMS). Acta Mater 48(1):179–196

Srikar VT, Spearing SM (2003a) Materials selection for microfabricated electrostatic actuators. Sens Actuators A 102(3):279–285

Srikar VT, Spearing SM (2003b) Materials selection in micromechanical design: an application of the Ashby approach. J Microelectromech Syst 12(1):3–10

Srinivasan P, Spearing SM (2008) Optimal materials selection for bimaterial piezoelectric microactuators. J Microelectromech Syst 17(2):462–472

Storgaard-Larsen T, Bouwstra S, Leistiko O (1996) Opto-mechanical accelerometer based on strain sensing by a Bragg grating in a planar waveguide. Sens Actuators A 52(1–3):25–32

Sugiyama S, Suzuki T, Kawahata K, Shimaoka K, Takigawa M, Igarashi I (1986) Micro-diaphragm pressure sensor. In: IEEE international electron devices meeting

Sun W, Chen X (2009) Preparation and characterization of polypyrrole films for three-dimensional micro supercapacitor. J Power Sources 193(2):924–929

Sun W, Zheng R, Chen X (2010) Symmetric redox supercapacitor based on micro-fabrication with three-dimensional polypyrrole electrodes. J Power Sources 195(20):7120–7125

Sundararajan AD, Hasan SMR (2014) Release etching and characterization of MEMS capacitive pressure sensors integrated on a standard 8-metal 130 nm CMOS process. Sens Actuators A 212:68–79

Swarnalatha V, Rao AVN, Pal P (2018) Effective improvement in the etching characteristics of Si{110} in low concentration TMAH solution. Micro Nano Lett 13(8):1085–1089

Taniuchi H, Umezawa H, Arima T, Tachiki M, Kawarada H (2001) High-frequency performance of diamond field-effect transistor. IEEE Electron Device Lett 22(8):390–392

Tsugai M, Hirata Y, Tanimoto K, Usami T, Araki T, Otani H (1997) Airbag accelerometer with a simple switched-capacitor readout ASIC. In: Micromachined devices and components III, International society for optics and photonics. 1997

Tu X-Z, Zemel JN (1993) Vertical-membrane optical-fiber pressure sensor. Sens Actuators A 39(1):49–54

Von Metzen RP, Stieglitz T (2013) The effects of annealing on mechanical, chemical, and physical properties and structural stability of Parylene C. Biomed Microdevice 15(5):727–735

Wagner C, Frankenberger J, Deimel PP (1993) Optical pressure sensor based on a Mach–Zehnder interferometer integrated with a lateral a-Si: H pin photodiode. IEEE Photonics Technol Lett 5(10):1257–1259

Wagner D, Frankenberger J, Deimel P (1994) Optical pressure sensor using two Mach–Zehnder interferometers for the TE and TM polarization. J Micromech Microeng 4(1):35

Wang X, Li B, Russo OL, Roman HT, Chin KK, Farmer KR (2006) Diaphragm design guidelines and an optical pressure sensor based on MEMS technique. Microelectron J 37(1):50–56

Wieczorek G, Schellin B, Obermeier E, Fagnani G, Drera L (2007) SiC based pressure sensor for high-temperature environments. In: 6th IEEE conference on sensors, 2007

Wilson SA, Jourdain RP, Zhang Q, Dorey RA, Bowen CR, Willander M, Wahab QU, Al-hilli SM, Nur O, Quandt E (2007) New materials for micro-scale sensors and actuators: an engineering review. Mater Sci Eng R: Rep 56(1–6):1–129

Wood JT, Embury JD, Ashby MF (1997) An approach to materials processing and selection for high-field magnet design. Acta Mater 45(3):1099–1104

Wur DR, Davidson JL, Kang WP, Kinser D (1995) Polycrystalline diamond pressure sensor. J Microelectromech Syst 4(1):34–41

Xue N, Gao G, Sun J, Liu C, Li T, Chi C (2018) Systematic study and experiment of a flexible pressure and tactile sensing array for wearable devices applications. J Micromech Microeng 28(7):075019

Yang X, Grosjean C, Tai Y-C (1999) Design, fabrication, and testing of micromachined silicone rubber membrane valves. J Microelectromech Syst 8(4):393–402

Yasukawa A, Shimada S, Matsuoka Y, Kanda Y (1982) Design considerations for silicon circular diaphragm pressure sensors. Jpn J Appl Phys 21(7R):1049

Yazdani M, Payam AF (2015) A comparative study on material selection of microelectromechanical systems electrostatic actuators using Ashby, VIKOR and TOPSIS. Mater Des 65:328–334

Yi T, Kim C-J (1999) Measurement of mechanical properties for MEMS materials. Meas Sci Technol 10(8):706-716

Zhou X-P, Deng R-S, Zhu J-Y (2018) Three-layer-stacked pressure sensor with a liquid metal-embedded elastomer. J Micromech Microeng 28(8):085020